LA-UR- 00-5334

Approved for public release; distribution is unlimited.

Title: LOW AMPLITUDE IMPACT TESTING OF BASELINE AND AGED, PRISTINE AND DAMAGED PBX 9501

Author(s): Deanne J. Idar, James W. Straight, Michael A. Osborn, William L. Coulter, Cary B. Skidmore, David S. Phillips, Michele E. DeCroix, Gregory A. Buntain, and Phillip M. Howess

Submitted to: JANNAF Combustion Subcommittee Air Breathing Propulsion Subcommittee/ Propulsion Systems Hazards Submcommitee/ Modeling and Simulation Subcommittee Joint Meeting, Nov. 13-17, 2000, Monterey, CA

Los Alamos
NATIONAL LABORATORY

DISCLAIMER

LOW AMPLITUDE IMPACT TESTING OF BASELINE AND AGED, PRISTINE AND DAMAGED PBX 9501

D.J. Idar, J.W. Straight, M.A. Osborn, W.L. Coulter,
C.B. Skidmore, D. S. Phillips, M. E. DeCroix, G.A. Buntain, and P.M. Howe

Los Alamos National Laboratory
P.O. Box 1663, Los Alamos, NM 87545

ABSTRACT

Low amplitude impact tests on pristine, aged and damaged PBX 9501 specimens were performed to determine the critical impact-velocity threshold for violent reactions as a function of initial state. Tests were performed with a 2 kg hemispherical spigot projectile launched from a powder driven gun at PBX 9501 in lightly confined Modified Steven targets. HE damage was achieved by a single impact ranging in velocity from 36.9 to 54.4 m/s. External blast gauge and ballistic pendulum data were used to evaluate reaction violence relative to a steady-state detonation. Velocity and impact timing were achieved with a photodiode velocity screen array and PVDF gauges. Strain gage data were used to evaluate the response of the explosive to impact and characterize subsequent reaction profiles. Polarized light microscopy, scanning electron microscopy, and second harmonic generation techniques were used to perform post-test characterization on remaining PBX 9501 specimens. Test results indicate that the pristine threshold between baseline and aged materials can slightly vary, attributed to density variations, and that the damaged threshold is lower than the pristine threshold while invariant to PBX 9501 lot-to-lot and age variables. Damaged materials show evidence of β to δ phase conversion in the HMX, mechanical damage to crystals, and evidence of bubble formation and melt layers.

INTRODUCTION

Low-velocity mechanical impact leading to unintentional reaction is of concern in accident scenarios involving the handling, transport, and storage of high explosives (HE). These have been investigated using different experimental techniques, from small- to large-scale, including, but not limited to the drop weight impact, Taylor anvil impact, Susan,[1] and more recently, the Steven and Modified Steven tests.[2-8] Ideally, the data will be used to further advance 3-D computational predictive capability in chemistry-based reaction models for the assessment of HE response to mechanical insult.

The challenges in this type of research are numerous and complex. The HE formulations vary in composition, density, porosity, and particulate distributions. These differences directly affect the HE behavior and degree of sensitivity. Confinement, environmental conditions and impactor characteristics also play a significant role in the behavioral response of the HE.

It is important to note that determining the best method to extrapolate the data to different dimension and mass scales further complicates data interpretation and usefulness. The key is to determine which are the most relevant parameters leading to ignition/reaction with a sensitive, reproducible test configuration and reliable diagnostic measurements in tandem with computational analyses.

Our overall objectives for these experiments were to (1) evaluate the HE reaction threshold behavior for aged PBX 9501 relative to baseline, and pristine versus damaged (2) characterize the degree of reaction violence relative to a detonation, (3) compare experimental results with past Modified Steven test data,[6] and (4) provide data to continue development of a reliable 3-D computational predictive capability. This report summarizes our single- and double-impact test results with baseline and aged PBX 9501 in Modified Steven targets. Target design, diagnostics, and relative reaction levels results are described.

EXPERIMENTAL

HIGH EXPLOSIVE, TARGET DESIGNS AND DIAGNOSTICS

Three different lots of PBX 9501 were used in these tests. PBX 9501 is a conventional high explosive formulation composed of 94.9/2.5/2.5/0.1 wt% of HMX, Estane 5703, a 1:1 eutectic mixture of bis(2,2-dinitropropyl)acetal [BDNPA] and bis(2,2-dinitropropyl)formal [BDNPF], and a stablizer/free radical inhibitor (either diphenylamine [DPA] or Irganox 1010). The HMX is a bimodal distribution of a three-to-one ratio of coarse-to-fine Class 1 and 2 grades. The Estane 5703 is an amorphous, thermoplastic polyester polyurethane with a glass transition temperature (T_g) of –31°C.[9] The addition of the BDNPA-F plasticizer causes the glass transition temperature to decrease ~13 to 18 degrees while increasing the flexibility and acting as a lubricant to promote the sliding of the polymer chains and reduce the degree of entanglement. The stabilizer/inhibitor reduces free radical reactions and mitigates molecular weight degradation of the Estane 5703.

The lot numbers, formulation year, average densities, and compositional analyses for the three library lots are given in Table 1. The lots differ in formulation age, density, and in composition. The oldest lot, HOL77J685-002 (hereafter referred to as 685-002), was stabilized with DPA and the other two lots, HOL81G730-005 and HOL89C730-010 (hereafter referred to as 730-005 and 730-010 respectively), with Irganox 1010. Lot 730-010, the youngest, was defined as the baseline lot for these tests. A comparison of the composition data and Estane molecular weights shows that lot 685-002 has the highest HMX and RDX weight percent, and the lowest molecular weight values for the Estane 5703.

The baseline PBX 9501 specimens were machined from samples pressed in 1997 and 1998. Aged specimens were obtained from Stockpile Laboratory Test (SLT) hemishells produced from lots 685-002 and 730-005. These were pressed in the late 1970s and early 1980s. The aged material was also denser than the baseline specimens. The aged specimens were installed in the targets to insure consistent orientation with the prior SLT orientation in mind. All of the specimens were machined to 5.0-in. diameter by 0.5-in. thick.

Table 1: PBX 9501 Library Lot Composition Data

	Aged Lot 685-002	Aged Lot 730-005	Baseline Lot 730-010
Formulation year	1977	1981	1989
Stockpile age	182 months	142 months	0 months
Ave. Density (g/cm^3)	1.840	1.840	1.830
HMX, wt%	95.0704 ± 0.1094	94.6925 ± 0.0017	94.8172 ± 0.0641
RDX, wt%	0.2388 ± 0.0274	0.0449 ± 0.0003	0.0006 ± 0.0001
Estane, wt%	2.4535 ± 0.0107	2.4566 ± 0.0193	2.4342 ± 0.0192
Estane Mw[a]	87093 ± 672	102553 ± 991	107665 ± 1001
Estane Mp[a]	85583 ± 1296	94841 ± 1200	97762 ± 1239
Estane Mn[a]	54783 ± 129	65372 ± 291	68284 ± 187
BDNPF, wt%[b]	0.9969 ± 0.0330	1.3568 ± 0.0056	1.2000 ± 0.0782
BDNPA, wt%[b]	1.1041 ± 0.0352	1.4140 ± 0.0073	1.1630 ± 0.0687
Stabilizer, wt%[c]	0.0597 ± 0.0014	0.0535 ± 0.0002	0.0695 ± 0.0065
PBNA, wt%	0.00331 ± 0.00011	0.00348 ± 0.00001	0.00330 ± 0.00026

[a]The Estane 5703 molecular weight data were determined using gel permeation chromatography (GPC) with a polystyrene standard in THF solution on the library lot specimens. The library lot specimens were stored as molding powder bagged in ~50 lb boxes in magazines without humidity or temperature control.
[b]The total wt% NP is equal to the sum of the BDNPA and BDNPF components.
[c]Lot 685-002 was formulated with diphenylamine (DPA) and the other two with Irganox 1010.

The basic target design started as a modification of the target assembly used in the original target series[6] and those used by Chidester et al.[2] with HE and target material constraints in mind. The design, as depicted in Figure 1 and described in Table 2, consisted of a holder, cover plate, and retaining ring. The PBX 9501 article was centered and covered with a 0.020-in. thick Sylgard 184 layer and the cover plate. The design allowed for an annular gap of 0.125-in. between the HE o.d. and the holder i.d. The

targets were assembled and secured to a mild steel backing plate, 12.0-in. square by 3.0-in. thick with a 0.75-in. deep cavity, which served as a high-impedance boundary.

Mild steel projectiles, 2 kg with a 3.0-in diameter hemispherical nose, traveling at velocities between 37 and 103 m/s were used for these tests. For this purpose, a unique spigot gun, using IMR 4350 powder, was designed to launch a shanked projectile, with the head external to the barrel. Further details of the gun design, the powder loads, and the velocities may be found in References 6 and 8, reports on the first and second series of experiments.

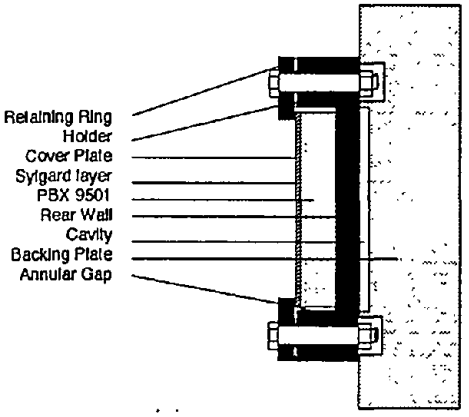

Figure 1: Basic Modified Steven target.

Table 2: Target design materials and dimensions.

Design	Cover Plate	Holder	Retaining Ring
Small, thin	304 stainless steel	A36 steel	A36 steel
	0.118±0.001-in. thick	5.250±0.005-in. i.d.	4.500 ±0.005-in. i.d.
	5.000±0.005-in. diameter	7.500±0.005-in. o.d.	7.500 ±0.005-in. o.d.
		0.638±0.002-in. deep	0.500 ±0.002-in. thick
		0.750±0.005-in. thick rear wall	

A cheap, easily replaceable light box/photodiode system was designed for determining the projectile velocity. Three halogen lights, each with a corresponding photodiode, were spaced at three-inch intervals in a wooden frame. The data records yield three light profiles producing two independent velocity measurements. A polyvinylidene flouride (PVDF) gauge was attached to the front surface of the target to record the projectile impact time. The guages have proved to be reliable, but are quite noisy and can cause interference on other diagnostic records. The impact timing provides an additional data point to evaluate the projectile velocity. This datum is averaged with the velocity data from the photodiode box.

One to two strain gauges were centered on target rear surface to record the deformation relative to the time of impact. With two gauges the elements were oriented at right angles to each other. Micro-Measurements EA-06-500BH-120 strain gauges amplified with Vishay 2311 signal conditioners were used for this purpose. Several iterations of gauge and lead wire mounting schemes were used to increase data collection time. The gauges and lead wires typically survived after the projectile impact and rebound, and were reused for the second impact tests. Data loss occurred when the gauges were either crushed between the back plate and the rear mounting block or when the cables were destroyed.

VIOLENCE OF REACTION/DELAY TO REACTION

Predicting the degree of violence of PBX 9501 reactions for a given reaction is desirable for risk assessments and a goal for computational models. A ballistic pendulum based on the classic design, and blast overpressure gauges were used to determine the violence of reaction relative to a PBX 9501

steady-state detonation. The two entirely different methods produced strikingly similar results, not only for high levels of reaction, but also for very low levels of reaction. The pendulum weight was adjusted to 2098 lb for the small targets by adding or removing 95-lb plates from the pendulum box. The mild steel backing plate added approximately another 110 lb to the overall weight. Momentum transfer calculations were performed for varying amounts of detonating PBX 9501 for two different pendulum weights. These were benchmarked with four PBX 9501 calibration charges. The degree of pendulum displacement was measured using two independent passive measurements: a friction pivot-arm that locks in place at the peak of the pendulum swing, and a thin cable, labeled with a marker, displaced by the pendulum swing. Tests that did not result in a violent reaction of the HE were described as quenched and/or damaged.

The blast overpressure gauge data were obtained with two PCB Piezotronics Inc. Model 102A15 transducers, 0-200 psi, in face-on mode positioned at 45° off of the projectile axis, at a distance of 10 ft from the front target face. Power to the transducers was provided by a PCB Piezotronics power supply. Output signals were coupled at 1-MΩ AC into LeCroy 9400A oscilloscopes. Pressure and timing calibrations were accomplished in tandem with the ballistic pendulum calibration tests. The blast gauge measurements were averaged with the ballistic pendulum data to determine an average energy release relative to a full detonation. The time interval between impact and violent reaction was estimated with two methods. The delay time was estimated from strain gauge records, and/or by comparison of the impact and blast wave timing.

POSTTEST TARGET CHARACTERIZATION

Eight of the first impact tests resulted in damaged targets. Each target was opened for nonintrusive evaluation and only one was evaluated with destructive methods. Only a brief summary of the posttest characterization methods will be provided here. These techniques and their results have been described in more detail by Phillips, and Skidmore, et al.[10, 11]

Nonintrusive techniques included dent/deformation measurements, visual examination of the PBX 9501 surface, and radiographs of the cracked PBX 9501. The dent data were used to validate the material models for the engineering codes. The front dent data were analyzed from depth measurements obtained from the top-to-bottom, and left-to-right axes on the front surface of the cover plates or the inside surface of the target assembly. Typically, if impact did not occur on center, the front dent data were measured twice, once through the impact point, and once through the center face of the target.

Visual examination of the HE top surfaces verified that the PBX 9501: (1) had deformed to fill the annular gap, and (2) displayed circumferential cracks around the impact diameter and radial cracks emanating from the impact point, with some evidence of material dislocation. An example of this can be seen in the images of the first target, K8-2147, impacted at 36.9 m/s as shown in Figure 2. Extensive posttest characterization was also performed on the PBX 9501 recovered from the fifth target K8-2174, impacted at 54.4 m/s, just below threshold velocity. Regions of the target where some level of reaction was indicated by fissures or cracks were the focus of the characterization. The principal techniques employed were polarized light microscopy (PLM) and scanning electron microscopy (SEM). That evaluation suggested the presence of re-solidified melt and other phases of HMX. Reflectance Fourier transform infrared (FTIR) spectroscopy, second harmonic generation (SHG),[12] and powder x-ray diffraction were used to confirm the presence of δ-phase HMX.

Two regions were sampled for PLM and SEM analysis. One was just under the impact point of the nose of the projectile. Here, there were indications of melt on the surface against the metal holder and just under the front HE surface. Dissection of the nose region revealed a path that connected with the principal fissure (radial). PLM analysis of the fissure region had similar indications that melt had occurred.

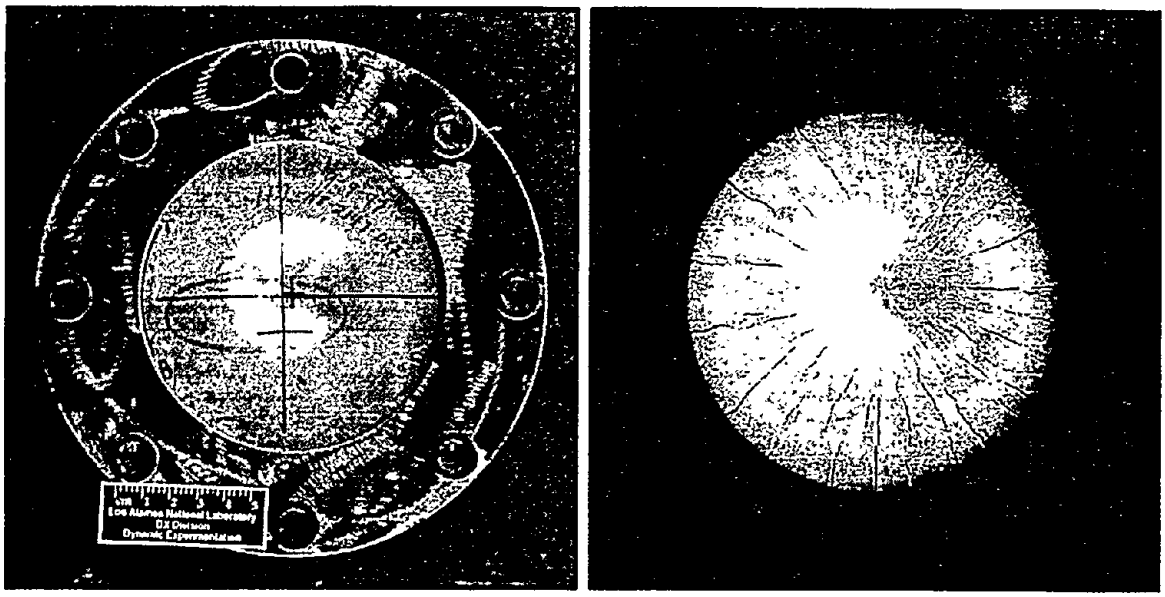

Figure 2: Images of target K8-2147 with and without the cover plate showing the front dent, and crack damage to the PBX 9501 after a 36.9 m/s impact.

Figure 3 shows a typical melt region in cross-section. Three layers are apparent. The top layer is of uniform contrast and appears to contain many facsimiles of bubbles, presumably formed by the evolution of decomposition gases while the melt was solidifying. The second layer is characterized by highly textured contrast in the region of a parent crystal nearest the first layer. This is indicative of a transition region between that which was melted and that which was not. The third layer, or parent material, resembles only mechanically damaged material

Figure 3. PLM image showing cross-section of melt region in impact zone. Impact was toward top of image.

The surface topology of a typical melt region is shown in Figure 4. There is an unmistakable lack of crystalline features as would be typical in a fracture specimen. Rather, the amorphous undulations and holes suggest a frothy melt that was quickly frozen, presumably by a suddenly quenched reaction This provides a strong corollary to the cross-section shown in the PLM image.

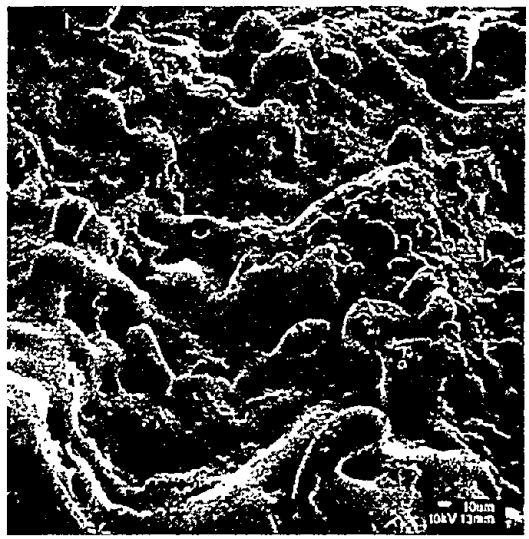

Figure 4. SEM image showing surface topography of melt in impact zone.

PLM and SEM images from this analysis were compared with those from samples of pressed HMX and PBX 9501 that were undisturbed mechanically, but which were burned by flame and quenched suddenly The conclusion is that for target K8-2174, the mechanical insult from a projectile impact resulted in damage to the PBX 9501 that is typical of solely a thermal insult

Posttest characterization is ongoing, and other techniques are being investigated to further characterize the damaged state of the PBX 9501. The surfaces of impact-damaged PBX 9501 also showed positive SHG effects, predominantly at the center of the impact location, in the open cracks, and in areas of shear dislocation. These preliminary analyses coupled with the FTIR reflectance and x-ray powder diffraction (XPD) confirmation data verify the existence of δ-phase HMX on the top surface of the damaged PBX 9501 up to 1 year after the initial impact.

MODELING

Calculations using the engineering models DYNA2D and SPRONTO have been performed to support these, and other, low-amplitude insult experiments. These are described in more detail by Scammon, et al [13] The DYNA2D finite element calculations employ an ignition criterion as a function of a characteristic constant, pressure, time, and the maximum shear strain rate to evaluate the threshold level for reaction The code was originally written with ignition and chemistry models derived from empirical fits to shock-to-detonation-transition (SDT) data, which does not match the mechanical ignition data well The SPRONTO code is a result of embedding the statistical crack mechanics model, SCRAM, into the mechanical deformation code PRONTO. It solves the one-dimensional heat equation, perpendicular to the planes of penny-shaped cracks, i.e., thin and oblong, excited into two-dimensional grinding motion by the impact, and computes the chemical response of the PBX 9501. These calculations allow us to study pressure and strain rates, to investigate structural aspects of the experiment, and to predict velocities required for reaction Structural analyses have played an active role in this project beginning with the original target design and continuing through analyses of the experimental results Alternative designs and various ideas for active instrumentation were examined as part of the experiment evolution process Predictions of reaction are used to guide these experimental design studies, even though we do not yet have enough experimental data to fully calibrate any of the models.

RESULTS AND DISCUSSION

The violent reaction of the HE from the first impact resulted in damage and deformation to the retaining ring and cover plate with slight deformation to the inside surface of the holder. No burn or scorch marks were evident on the holder or cover plate in these tests. This is a lower degree of damage than previously witnessed in the large, thick targets described previously reported.[6] This can possibly be attributed to the smaller mass of PBX 9501. This assumption is further supported by the average energy release, which never exceeded 41±6% for this target size. Small pieces of PBX 9501 were recovered from each of the reactive events, decreasing in quantity as the projectile velocity was increased. The test numbers, projectile impact velocities, and average energy release data are given in Table 3.

An examination of the strain gauge records (figure 5) provides additional insight regarding the reaction behavior. The back plate strain gauge records show a strong consistency in the impact-induced reaction sequence. The explosive initially behaves as an elastic-solid, transmitting force to the back plate. Near 2000 microstrain at the back plate, the explosive starts to crush and flow radially. The force levels off and then starts to decrease as the explosive crushes until the annular gap is filled and the pressure on the crushed explosive begins to increase again. A comparison of the data also shows that the delay, ranging from approximately 200 to approximately 400 μs, between impact to violent reaction decreases as the projectile velocity increases.

Table 3: Test data for first impact tests.

Test #	Test Date	PBX 9501 lot [a]	Density (g/cm^3)	Projectile Velocity (m/s)	Test Result	Average Energy Release
K8-2147	09/09/97	730-010 [a]	1.830	36.9 ±0.8	Quenched	0%
K8-2150	09/12/97	730-010 [a]	1.830	49.4 ±1.1	Quenched	0%
K8-2168	10/07/97	730-010 [a]	1.831	51.8 ±1.2	Quenched	0%
K8-2165	09/30/97	730-010 [a]	1.831	52.7 ±1.2	Quenched	0%
K8-2174	10/14/97	730-010 [a]	1.830	54.4 ±1.3	Quenched	0%
K8-2171	10/07/97	730-010 [a]	1.830	55.9 ±1.3	Violent reaction	16.1 ±0.3%
K8-2162	09/30/97	730-010 [a]	1.831	57.9 ±1.3	Violent reaction	32.7 ±2.3%
K8-2159	09/23/97	730-010 [a]	1.830	68.9 ±1.6	Violent reaction	34.0 ±2.2%
K8-2156	09/18/97	730-010 [a]	1.831	74.4 ±1.7	Violent reaction	35.9 ±2.4%
K8-2153	09/16/97	730-010 [a]	1.830	77.7 ±1.8	Violent reaction	37.9 ±1.6%
K8-2178	10/28/97	730-005 [b]	1.840	45.0 ±1.0	Quenched	0%
K8-2300	11/14/97	685-002 [b]	1.840	48.0 ±1.1	Quenched	0%
K8-2180	10/28/97	730-005 [b]	1.841	51.8 ±1.2	Quenched	0%
K8-2183	11/04/97	730-005 [b]	1.840	53.0 ±1.2	Violent reaction	17.9 ±0.4%
K8-2176	10/14/97	730-005 [b]	1.840	54.3 ±1.2	Violent reaction	41.2 ±5.7%
K8-2297	11/04/97	685-002 [b]	1.840	54.4 ±1.3	Violent reaction	21.4 ±2.2%
K8-2303	11/18/97	685-002 [b]	1.840	55.1 ±1.3	Violent reaction	36.0 ±1.4%
K8-2306	11/18/97	685-002 [b]	1.841	103.0 ±2.4	Violent reaction	39.9 ±0.5%

[a]Baseline tests, and [b] aged tests.

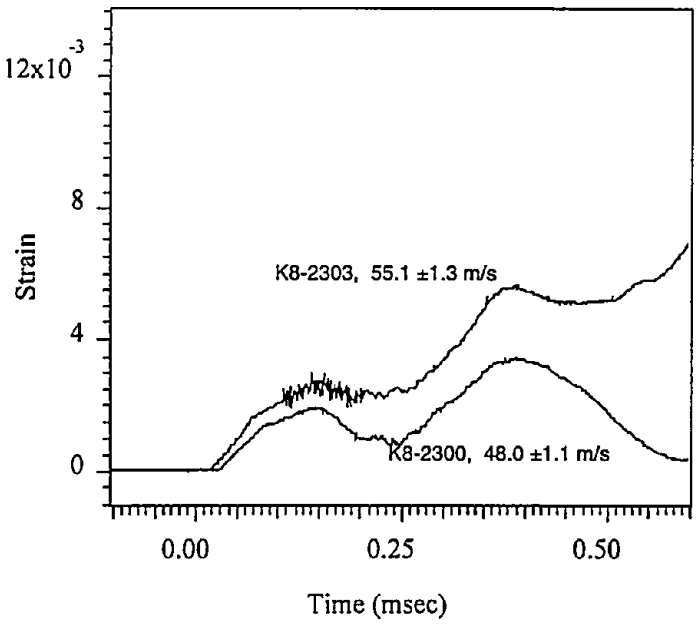

Figure 5: Examples of strain gauge records from tests K8-2300 and K8-2303. Test K8-2303 resulted in a violent reaction, and test K8-2300 was quenched.

Strain gauge results suggest that high impact velocities result in fast build-up to reaction achieving critical pressures that result in violent reaction with damage to the target. At slower velocities, the build-up is slower, and the target confinement is able to rapidly relieve the pressure and quench the reactive event. Consequently the HE is only damaged and the projectile simply rebounds, releasing the force on the back plate. Because these strain-gauge records clearly show the mechanical behavior and reaction timing of the explosive, they become excellent data for benchmarking the computer codes. As expected, the strain gauge data show the delay to violent reaction relative to impact time decreases as the projectile velocity is increased. At velocities much greater than threshold, the strain records show that the reactive event occurs even before the force on the back plate begins to decrease.

Semiquantitative delays in reaction times can also be determined by comparing the blast gauge time profiles with impact times. The diagnostic data indicates delay times in the blast wave arriving at the gauges decreasing from 2.8 to 1.3 m/s as the projectile velocity is increased to approximately 103 m/s.

The threshold behavior (see Figure 6) for the small, thin targets demonstrates the same sharp consistency as seen with the large, thick targets of the original test series. The data also do not demonstrate evidence of mixed zone (crossover) results, i.e., violent reactions at lower velocities than the threshold, or nonviolent events at higher velocities that exceed the threshold. Threshold velocities ranged from 54.4 to 55.9 m/s and from 51.8 to 53.0 m/s for the baseline and aged targets, respectively. Based on this threshold shift, it is important to examine possible differences between the baseline and aged PBX 9501 lots.

A review of the data in Table 1 shows differences in the compositional and GPC analyses of the PBX 9501 library lots, notably weight percent of RDX, the weight percent sum of the NP, the molecular weight of the Estane 5703, and in density. The relative effect of each of these on the threshold response has not been verified. The density difference, 0.01 g/cm^3, may first appear to be insignificant. The calculated theoretical maximum density (TMD) for PBX 9501 is 1.860 g/cm^3. The specimens tested here ranged from 98.4 to 98.9% TMD. If the remaining percentage is attributed to porosity, the difference between the two densities is significant. Porosity may play a key role in the time-dependent energy dissipation in the HE after impact.

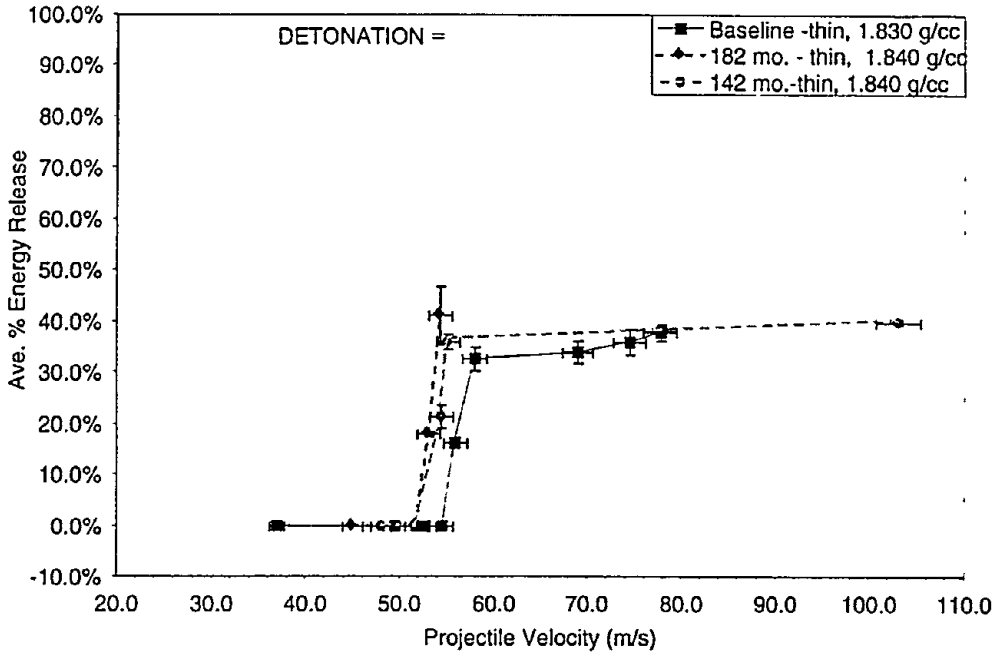

Figure 6: Reaction threshold data for the pristine, baseline and aged Modified Steven targets.

The effect of density on mechanical ignition events is being explored further with lab-scale, quasi two-dimensional tests.[13] The initial test results from these experiments show a higher shear strain rate in the 1.830 g/cm^3 PBX 9501 specimen compared with the 1.820 g/cm^3 specimen when impacted under identical conditions. The Steven test threshold differences between the baseline and aged data are postulated to be due to the differences in densities.

Interestingly, the threshold velocity range for the small, thin targets could be correlated with a pinch of the PBX 9501 between the cover plate and rear surface of the holder. In these tests, the impact of the projectile deforms the cover plate to the extent that it comes in direct contact (pinch) with the inside surface of the holder. This was evident by the circular impact markings on the inside surfaces of the cover plate and holder. Further, a linear regression fit to the projectile velocity as a function of the measured dent of the quench targets depths (with the exception of test K8-2174) allows one to extrapolate to a velocity where the PBX 9501 thickness will be fully pinched. This fit corresponded to a velocity of 54.7±0.5 m/s.

Seven of the eight remaining damaged targets were reassembled for the second impact tests, which were performed in the same manner as the first impact tests. The velocities and results are given in Table 4. The HE violent reaction from the second impact tests were similar to the first impact test results. The retaining ring and cover plate were damaged and deformed, and the holder was only slightly deformed by the violent reaction. No burn or scorch marks were evident on the holder or cover plate, and the average energy release did not exceed 40±2%.

An examination of the strain gage records provides additional insight regarding the reaction behavior (see Figure 7.) Initially pressure increases on the damaged explosive as the impact crushes it further, and either leads to a very violent reaction, or a quenched event. A comparison of these data also shows that the delay between impact to violent reaction decreases as the projectile velocity increases.

A review of the damaged threshold data (see Figure 8), from 32.2 to 34.0 m/s, shows a significant reduction, ~41%, relative to the pristine material threshold. This trend is consistent with similar studies by Chidester, et al.[6] Whether or not the reduction in threshold is due to the damaged HE being pinched, increased surface area, the presence of the delta HMX polymorph plus thermally induced damage, and/or other factors remains to be determined. Despite the shift, the threshold behavior demonstrates the same

sharp consistency without evidence of mixed zone results. Remarkably, the data also show that 1) the damaged threshold in this test configuration does not display a variable dependence on the molding powder formulation age, pressing age, lot-to-lot variation, or prior level of damage in the PBX 9501, and 2) the highest energy release in the damaged targets does not exceed the that in the pristine targets. Further research is still required to evaluate the effect of damage and other variables on threshold sensitivity.

TABLE 3: Test dates, projectile velocity, and average energy release data.

1st Test #	1st Test Date	PBX 9501 lot [b]	1st Projectile Velocity (m/s)	2nd Test #	2nd Test Date	2nd Projectile Velocity (m/s)	Average Energy Release
K8-2174[a]	10/14/97	730-010	54.4 ±1.3	—	—	—	—
K8-2168	10/07/97	730-010	51.8 ±1.2	K8-2788	09/30/98	28.6 ±0.7	0.0%
K8-2300	11/14/97	685-002	48.0 ±1.1	K8-2776	07/30/98	31.6 ±0.7	0.0%
K8-2147	09/09/97	730-010	36.9 ±0.8	K8-2782	09/16/98	32.2 ±0.8	0.0%
K8-2180	10/28/97	730-005	51.8 ±1.2	K8-2773	07/23/98	34.0 ±0.8	28.9 ±0.3%
K8-2150	09/12/97	730-010	49.4 ±1.1	K8-2785	09/30/98	36.1 ±0.8	31.3 ±2.1%
K8-2178	10/28/97	730-005	45.0 ±1.0	K8-2770	07/15/98	38.0 ±0.9	36.6 ±8.7%
K8-2165	09/30/97	730-010	52.7 ±1.2	K8-2791	12/02/98	106.0 ±2.4	40.4 ±2.3%

[a]Target K8-2174 was selected for destructive post-test characterization techniques.
[b]Lot 730-010 was used in the baseline targets, and lots 685-002 and 730-005 were used in the aged targets.

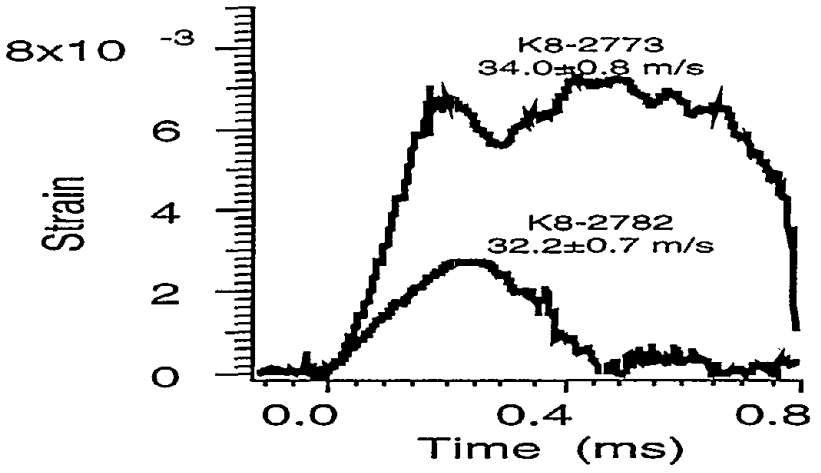

Figure 7. Strain versus time for second impact tests K8-2773 and K8-2782.

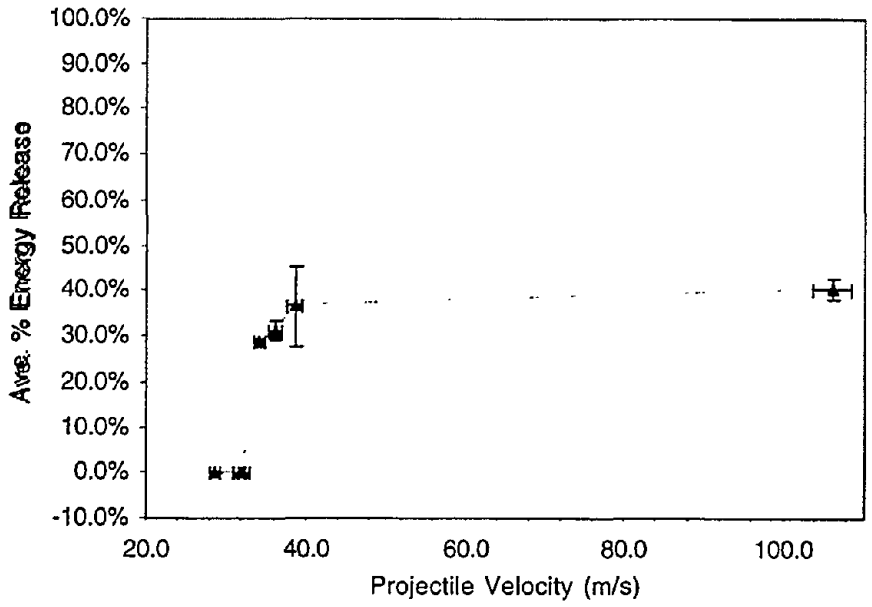

Figure 8: Reaction threshold data for the damaged, baseline and aged Modified Steven targets.

SUMMARY

The mechanical loading behavior and response of PBX 9501 have been investigated using modified Steven target designs. Low-velocity impact was achieved by launching a mild-steel spigot projectile with a powder-driven gun design at PBX 9501 in lightly confined steel targets. The threshold velocities for reaction and violence of reaction for different PBX 9501 lots and histories were evaluated and compared.

Various diagnostics were used to record the timing and target strain behavior relative to projectile impact. The strain gauge records provide evidence for a sequence of events as follows: low-pressure impact, HE material failure, followed by recompaction of the damaged HE, which results in either violent reaction or a quenched event. The gauge data also show that the time scale for the target destruction decreases as a function of increasing projectile velocity.

The physical target evidence and the predictable pinch calculated from the dent profiles of the small, thin targets, suggest that ignition occurs directly under impact. Further work is required to verify this hypothesis.

The violence of reaction, as measured by both passive and active techniques, is reported relative to a detonation in PBX 9501. The recorded violence was never equivalent to a complete detonation of the PBX 9501 and was always delayed relative to a prompt detonation. The highest average energy release recorded was approximately 41 ±6%. This is lower than the highest average energy release recorded for the large, thick targets of roughly 67±4%.

Posttest characterization of the PBX 9501 quenched and reacted targets is ongoing. Preliminary analysis with PLM and SEM techniques displays evidence of permanent stress-induced twinning in the HMX crystals, melt layer zones, and evidence of gas evolution on the melt layer surface most likely due to reaction. SHG, FTIR, and XPD evidence also shows that a beta to delta HMX phase transformation has occurred on the surface of the damaged PBX 9501. This provides evidence for a thermal excursion induced by the impact.

Two- and three-dimensional modeling with DYNA2D, SPRONTO, and DYNA3D is concurrent with the experimental work. The calculations have been instrumental in the evolution of the experimental design and testing methods. Front dent deformation data have been used to calibrate the material models for the calculations. Experimental strain and pressure profiles are also being used to benchmark the calculations.

Both the baseline and aged target series in pristine and damaged states have demonstrated a remarkably sharp threshold to reaction without evidence of mixed zone results (crossovers). The stockpile-aged samples showed a slight decrease in reaction threshold relative to baseline results. This may be due to the slightly higher densities of the aged materials, variations in the composition, e.g., RDX weight percent, and/or particle size distributions. The damaged HE threshold shows a significant decrease in velocity relative to pristine material, which may be due to several different factors, including but not limited to increased surface area, the presence of the delta HMX polymorph plus thermally induced damage, and/or other factors that remain to be determined.

Further work is required (1) to verify the ignition locus(ci); (2) to characterize the relative effect of the different projectiles, HE, and confinement variables on the threshold behavior, i.e., an increase or decrease in threshold; and (3) to determine a semiquantitative relationship for the threshold behavior as a function of the different variables.

ACKNOWLEDGEMENTS

We gratefully acknowledge the support of the following groups and individuals in these research activities: programmatic and technical support -Phil Howe, George Hurley, and Luis Salazar; analytical modeling support -Dick Scammon, Richard Browning, John Dienes, and John Middleditch; and x-rays and radiographic numerical analyses - Phil Berry, Greg Cunningham and Jim Harsh. We also thank Steve Chidester of Lawrence Livermore National Laboratory for his helpful suggestions regarding this research.

REFERENCES

1. L. G. Green and G. D. Dorough, "Further Studies on the Ignition of Explosives," Fourth International Detonation Symposium, ARC-126, Office of Naval Research - Department of the Navy, Washington, D.C. p. 477–486, 1965.
2. S. K. Chidester, L. G. Green, and C. G. Lee, "A Frictional Work Predictive Method for the Initiation of Solid High Explosives from Low-Pressure Impacts," Tenth International Detonation Symposium, Office of Naval Research, Arlington, Virginia , p. 786–792, 1993.
3. S. K. Chidester, C. M. Tarver, and C. G. Lee, "Impact Ignition of New and Aged Solid Explosives," 1997 American Physical Society Topical Conference on Shock Compression of Condensed Matter, AIP Conference Proceedings 429, Woodbury, New York, p. 707-710, 1997.
4. S. K. Chidester and C. M. Tarver, "Safety of Stockpile Aged Energetic Materials," 1998 Life Cycles of Energetic Materials, Fullerton, CA, Mar. 29–Apr. 1, 1998.
5. S. K. Chidester and C. M. Tarver, "Low-Amplitude Impact Testing and Analysis of Pristine and Aged High Explosives," Eleventh International Detonation Symposium, Snowmass, CO, Aug. 31–Sept. 4, 1998.
6. D. J. Idar, R. A. Lucht, R. J. Scammon, J. W. Straight, and C. B. Skidmore, "PBX 9501 High Explosive Violent Response/Low Amplitude Insult Project: Phase I," Los Alamos National Laboratory report LA-13164-MS (January 1997).
7. D. J. Idar, R. A. Lucht, J. W. Straight, R. J. Scammon, R. V. Browning, J. Middleditch, J. K. Dienes, C. B. Skidmore, and G. A. Buntain, "Low Amplitude Insult Project: PBX 9501 High Explosive Violent Reaction Experiments," Eleventh International Detonation Symposium, Snowmass, CO, Aug. 31–Sept. 4, 1998.
8. D. J. Idar, J. W. Straight, M. A. Osborn, C. B. Skidmore, D. S. Phillips, and G. A. Buntain, "PBX 9501 High Explosive Violent Reaction: Phase II Baseline and Aged Experiments," Los Alamos National Laboratory Report: LA-13641-MS, April 2000.
9. "Adhesives Technology of Estane Polyurethane," B. F. Goodrich Specialty Chemicals, TSR 76-02 TF116, March 1995.
10. D. S. Phillips, C. B. Skidmore, D. J. Idar, S. F. Son, R. B. Schwarz, and B. W Asay, "Defect Structures in Some Insulted HMX Composites," Inter/Micro 98, Chicago, ILL, Aug. 10–14, 1998.
11. C. B. Skidmore, D. S. Phillips, D. J. Idar, and S. F. Son, "Characterizing the Microstructure of Selected High Explosives," Europyro '99, Brest, France, June 7–11, 1999.

12. B. F. Henson, R. K. Sander, S. F. Son, J. M. Robinson, P. M. Dickson, and, B. W Asay, "Measurement of the HMX _-to-_ Phase Transition by Second Harmonic Generation," Phys. Rev. Lett. Vol 82(6) pp. 213-216. (May 1998).
13. R. J. Scammon, R. V. Browning, J. Middleditch, J. K. Dienes, K. S. Haberman, and J. G. Bennett, "Low Amplitude Insult Project: Structural Analysis and Prediction of Low Order Reaction," Eleventh International Detonation Symposium, Snowmass, CO, Aug. 31–Sept. 4, 1998.
14. B. W Asay, P. M. Dickson, B. Henson, C. S. Fugard, D. J. Funk, and D. J. Idar, "Dynamic Measurement of the Influence of Projectile Radius and Velocity on Strain Localization During Impact of an Energetic Material,"